Mars Exploration Rover Cruise Orbit Determination

Brian Portock*, Darren Baird†, Eric Graat‡, Joseph Guinn§, Tim McElrath**, Michael Watkins††, and Geoffrey Wawrzyniak‡‡
Jet Propulsion Laboratory, California Institute of Technology, Pasadena, California, 91109

The Mars Exploration Rover project consisted of two missions (MER-A: spirit rover and MER-B: opportunity rover) that launched spacecraft on June 10, 2003, and July 8, 2003, respectively. The spacecraft arrived at Mars approximately seven months later on January 4, 2004, and January 24, 2004. These spacecraft needed to be precisely navigated to a Mars atmospheric entry flight path angle of –11.5 deg ±0.12 deg (3σ) for MER-A and ±0.14 deg (3σ) for MER-B in order to satisfy the landing site delivery requirements. The orbit determination task of the navigation team needed to accurately determine the trajectory of the spacecraft, predict the trajectory to Mars atmospheric entry, and account for all possible errors sources so that the each spacecraft could be correctly targeted using five trajectory corrections along the way. This paper describes the orbit determination analysis which allowed MER-A to be targeted using only four trajectory correction maneuvers to an entry flight path angle of –11.49 deg ±0.010 deg (3σ) and MER-B to be targeted using only three trajectory correction maneuvers to an entry flight path angle of -11.47 ±0.021 deg (3σ).

Nomenclature

ΔV	=	delta velocity
$B\ R$	=	component of B-vector (hyperbolic miss vector) along R axis
$B\ T$	=	component of B-vector (hyperbolic miss vector) along T axis

I. Introduction

AFTER three years of development the first Mars Exploration Rover (MER) mission known as MER-A began with the lift-off of its spacecraft containing the rover Spirit. Just under one month later the second Mars Exploration Rover mission, known as MER-B launched carrying the rover Opportunity into orbit on its way to Mars. Immediately after each spacecraft separated from the launch vehicle third stage each spacecraft started sending a radio signal to Earth. The MER orbit determination analysts began work to determine each orbit toward Mars. The primary goal of the navigation team was to accurately deliver each spacecraft to the desired landing site. In order to deliver the spacecraft to the correct landing site the orbit determination analysts on the navigation team needed to reconstruct the trajectory of the spacecraft very accurately using radiometric tracking data and they needed to predict the trajectory to the atmospheric entry conditions. Satisfying the conditions at atmospheric entry was required so that each spacecraft would land in the

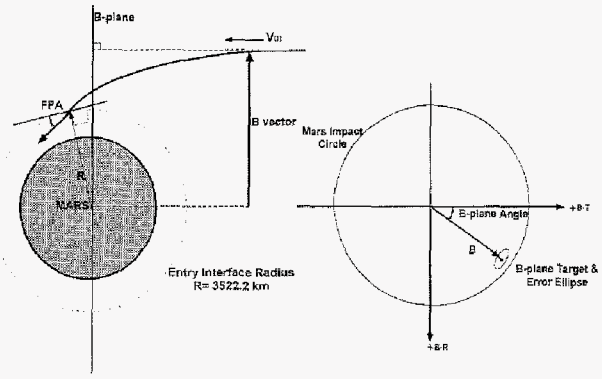

Figure 1. Flight Path Angle and B-plane Diagram[1]

---

* Member Engineering Staff, Navigation and Mission Design, M/S 301-276 4800 Oak Grove Blvd, AIAA Professional Member.
† Member Engineering Staff, Navigation and Mission Design, M/S 301-276 4800 Oak Grove Blvd, AIAA Professional Member.
‡ Mission System Manager, Phoenix Project, Design, M/S 301-276 4800 Oak Grove Blvd, AIAA Professional Member.
§ Member Engineering Staff, Navigation and Mission Design, M/S 264-380 4800 Oak Grove Blvd.
** Group Supervisor, Navigation and Mission Design, M/S 301-276 4800 Oak Grove Blvd.
†† Mission System Manager, Mars Science Laboratory Project, Design, M/S 301-125L 4800 Oak Grove Blvd.
‡‡ Member Engineering Staff, Navigation and Mission Design, M/S 301-276 4800 Oak Grove Blvd, AIAA Professional Member.

designated safe landing site. The entry conditions consisted of inertial entry flight path angle (FPA), B-plane angle, and entry time at a defined Mars entry radius (3522.2 km). Figure 1[1] shows entry FPA along with B-plane relative to Mars. The B-plane is the plane through the center of Mars that is perpendicular to the incoming V-infinity vector of the spacecraft and contains defined axes known as B R and B T. The FPA being the most important of the entry conditions controls the hypersonic path though the atmosphere, which determines most of the down-track travel to the landing point. The B-plane angle mostly controlled the entry and landing latitude due to the landing sites being close to the equator, and entry time controlled the entry and landing longitude. The landing point and landing uncertainty were by far the most sensitive to variations and uncertainty in the entry FPA, therefore the FPA was required to be –11.5 deg ±0.12 deg (3σ) for MER-A and ±0.14 deg (3σ) for MER-B. This paper will describe the results of the orbit determination (OD) process for each mission, MER-A and MER-B, during their transit to Mars ending with their final approach to Mars atmospheric entry.

II. Launch Orbit Determination

The purpose of OD directly after launch is to aide the Deep Space Network (DSN) in acquiring the initial signals from the spacecraft after it separates from the launch vehicle. The initial acquisition of signal is generally based on the launch vehicles predicted trajectory. The navigation team receives state estimates from the launch vehicle's telemetry at multiple points during the launch trajectory. This data is analyzed and can be used to aide the DSN in antenna pointing and acquiring the signal. Even if the initial spacecraft signal is acquired nominally, the trajectory needs to be determined such that the angular position of the spacecraft is known to ±0.032 deg (the 34 m station –3 dB half-cone beamwidth) at the second DSN station acquisition or the launch vehicle injection errors would grow to the point that the next DSN complex attempting to acquire the signal may be unsuccessful, which could cause a mission failure. The primary job of the OD analysts on the navigation team after launch is to update the spacecraft trajectory based on angle, Doppler, and range data to guarantee signal acquisition at the second DSN station rise.

A significant challenge of launch phase OD is the limited analysis time, which for the MER mission was between three and four hours before an updated trajectory had to be delivered to the DSN for the second station acquisition. To reduce solution execution time, elaborate data conditioning and filter configuration strategies were avoided. Both MER spacecraft had spin-rates within 12 ±2 rpm at the time of separation from the launch vehicle. Removal of the spin signature in the Doppler data was not performed for launch. The MER-A two-way Doppler data was weighted at the spin envelope level of 0.140 Hz at a ten second count time. The MER-B two-way Doppler data was optimally compressed by the spin period to decrease the data noise which yielded 0.003 Hz at a eighty-nine second count time. The range and angle data for both missions were weighted at four meters or less and 0.1 or less respectively. MER-B employed the use of difference one-way data to further reduce the orbit uncertainty at the second station rise. The technique of differencing two one-way Doppler signals from two DSN stations removed common errors sources and produced another data type that was weighted at 0.003 Hz similar to two-way Doppler data. This data was important for the time period before receipt of the two-way data and would have been extremely important if two-way data was unavailable in anomalous circumstances. Due to the circular polarization of the signal, a two-way Doppler bias of 0.4350 +/- 0.0725 Hz was estimated in the filter. The sign ambiguity of the spin-bias was resolved by including range data in the orbit solution. DSN station specific range biases were estimated in the filter as well. The estimated parameters in the filter were limited to spacecraft state, data biases and a single three-axis non-gravitational acceleration. Solutions fitting various combinations of data types were analyzed and compared (e.g. Doppler only vs. Doppler and range, etc.) before a single solution was selected for delivery to the DSN.

In the case of the MER-A and MER-B launches, no action was taken based on the launch vehicle telemetry data. The DSN successfully acquired the signal from each spacecraft within minutes of the predicted time. At the time of signal acquisition, angle data and one-way Doppler data were collected. After the operations team established a two-way coherent link with the spacecraft, two-way Doppler began being collected. Finally after the spacecraft was deemed to be in a nominal state, two-way ranging was established. Using this data and trajectory models, the angular positions of MER-A and MER-B were determined such that the second station acquisition went smoothly.

III. Mid-cruise Orbit Determination

The primary purpose of cruise orbit determination is to reconstruct the spacecraft trajectory in the past and predict it forward to Mars in support of trajectory correction maneuvers (TCMs) which target the atmospheric entry conditions and landing site. The orbit determination process supported three TCMs during the cruise phase for each

mission. Prior to each TCM, tracking data was maintained, the OD filter was tuned, and trajectory models were updated to insure the accuracy of the OD solutions.

The first TCM (known as TCM-A1 for MER-A and TCM-B1 for MER-B) primarily removed the launch vehicle injection bias and launch vehicle injection errors. TCM-A2 and TCM-B2 mainly clean up from TCM-1 execution errors. Similarly TCM-A3 and TCM-B3 correct OD and execution errors from TCM-2. The nominal time for TCM-1 on both missions was ten days after launch. The TCM design cycle for TCM-1 was five days long allowing time for orbit determination, maneuver design, maneuver implementation, testing, and uplink of commands. This allowed five days of collecting tracking data that would be used in the orbit determination process. That data consisted of nearly continuous two-way Doppler and ranging data starting just after launch. The nominal filter that used for the TCM-1 OD process was not very similar to the launch filter due to the shortness of the data arc and lack of dynamics that took place during that time. The only major planned event was a spin-down maneuver. This maneuver decreased the spin rate from 12 rpm to 2 rpm by using thrusters causing a trajectory ΔV because of misalignments and imbalances. The rest of the filter consisted of data assumptions such as data weights and range biases. The spacecraft spin rate caused a signature and a bias in the Doppler data that was dealt with by either compressing the data to the period of the spin signature, effectively removing the signature, or by estimating the spin using the data and removing it directly before the OD filter process.

The TCM-A1 OD data cut-off took place on July 13, 2003, five days before the scheduled TCM would take place. The two-way Doppler data was compressed to 89.7 seconds per point prior to the spin-down maneuver. After the spin-down maneuver the two-way Doppler data was compressed to 58.3 seconds to remove the spin signature. Down sampling the data by the spin period removes the spin signature by effectively averaging the signature of a full cycle down to a single point. As long as the signature is constant relative to the noise level the signature will be removed. Figure 2 shows the data with and without the spin signature. Spacecraft nutation caused by separation and the spin down maneuver did cause some uncorrected noise in the spin-removed data.

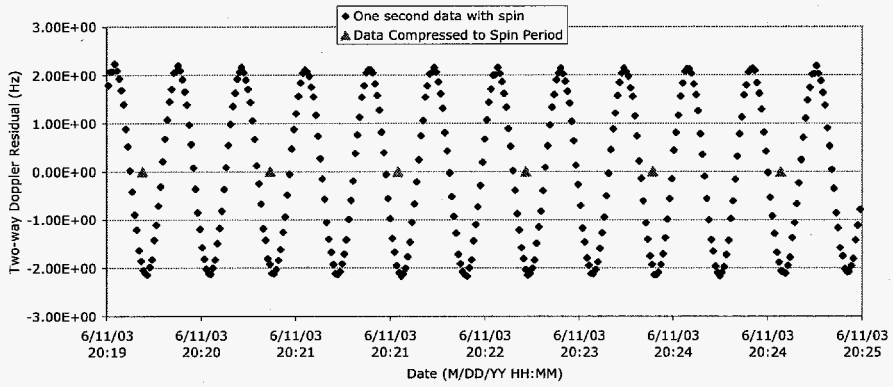

Figure 2. Two-way Doppler Data with and without Spin Signature

The MER-A filter was changed compared to the nominal plan based on the existence of a nongravitational acceleration acting on the spacecraft. The acceleration was estimated using two models: an exponential decaying acceleration model and a stochastically varying acceleration model. The stochastic model was used to deal with the quickly varying acceleration that existed directly after launch. The exponential model was used for a slower varying acceleration that was evident a day after launch. These models were used based on the theory that this acceleration was due to the release of material from the surfaces of the spacecraft lit by the sun. This is a process known as out-gassing, which has been witnessed directly after launch on other spacecraft. The estimated acceleration profile can be seen in Figure 3. The model worked well to fit the data as can be seen in Figure 4. The final OD solution prior to TCM-A1 predicted that the launch vehicle injected the spacecraft into a trajectory that was just over 255,000 km from the biased B-plane target and off in time of arrival by just over 1.7 days, which is less than a one σ error based on the predicted launch vehicle B-plane errors2. The OD B-plane uncertainty of the TCM-A1 solution was ± 791 km (1σ) in B R, ±1097 km (1σ) in B T, and ±1282 seconds (1σ) in the time of closest approach (TCA). The OD errors in the B-plane were small compared to the correction needed to remove the bias and injection errors. Further TCM-1 results for each spacecraft are included in Table 1 along with TCM-2 and TCM-3 results.

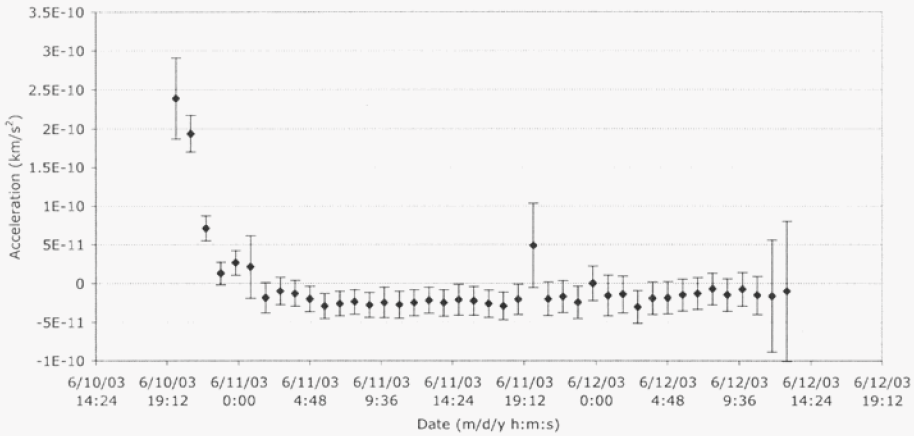

Figure 3. MER-A estimated acceleration directly after launch due to spacecraft out-gassing

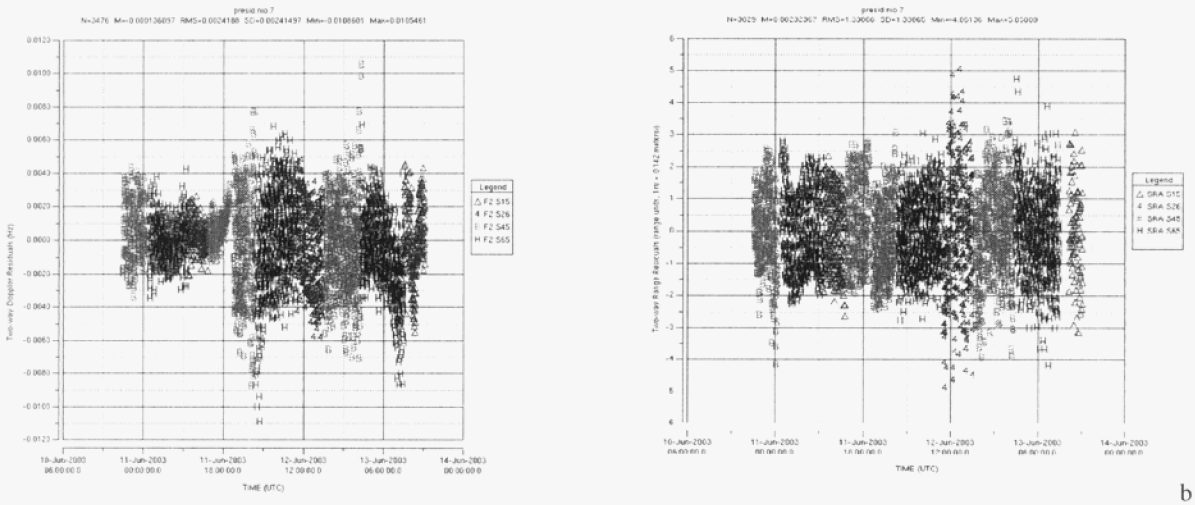

a b

Figure 4. a. Shows the two-way Doppler residuals when not estimating for the out-gassing acceleration b. Shows the two-way Doppler residuals when estimating for the out-gassing accelerations

The MER-B OD was deemed stable enough just three days after launch to use a data cut-off on July 11, 2003. This allowed more time (seven days) for the rest of the maneuver design cycle. Contrary to MER-A the spin signature in the Doppler data on MER-B was removed by estimating the spin using the data. Similar to MER-A, MER-B also experienced acceleration due to out-gassing. The same exponential acceleration model was used to fit the MER-B data. The MER-B OD solution prior to TCM-B1 predicted that the launch vehicle put the spacecraft into a trajectory that was just under 183,000 km away from the biased target and just over 0.1 days early in time of flight. This marks about a one and a half σ injection based on the predicted launch vehicle B-plane error[1]. The OD B-plane uncertainty of the TCM-B1 solution was ± 607 km (1σ) in B R, ± 986 km (1σ) in B T, and ±716 seconds (1σ) in TCA

The second and third maneuvers for each mission were purely statistical maneuvers - they cleaned up OD and execution errors from the previous maneuvers. TCMs two and three were planned to take place at launch plus sixty days and entry minus sixty days allowing each mission to use longer data arc for their final OD solutions. Long data arcs allow the OD process to refine trajectory and data models and therefore predict the future trajectory more accurately. The two major trajectory models we began to estimate for TCM-2 and further for TCM-3 were the solar

radiation pressure model and the ΔV due to turns. The data models that were incorporated included the addition of delta-differential one-way ranging (ΔDOR) data and the identification of a DSN tracking station location error. The results of the improved modeling insured that the OD knowledge prior to each of the cruise TCMs was significantly smaller than the amount of correction made by the maneuvers. The OD and TCMs performed so well for MER-B that TCM-B3 was canceled. A summary of the OD solutions prior to each TCM are found in Table 1.

Table 1: Cruise TCM OD Results

	MER-A			MER-B		
TCM	A1	A2	A3	B1	B2	B3 canceled
B R knowledge (km)	2375	1140	38	1822	237	-
B T knowledge (km)	3291	1584	42	2960	350	-
TCA knowledge (sec)	1282	691	17	716	107	-
B R correction (km)	-291824	-911	-426	-203730	-3122	-
B T correction (km)	-400839	-666	-644	-267418	-4772	-
TCA correction (sec)	-215412	-24416	-996	-127787	2793	-

The spacecraft needed to perform turns every so about once per month to keep the communication antenna pointing at Earth and the solar arrays pointed close to the Sun. The turns are done with a set of balanced thrusters, but miss-alignments and center of mass uncertainty imparted ΔV during the event. Prior to launch, analysis showed that this ΔV was could be as much as 3 mm/sec (1σ), which was high enough to make it one of the most significant error sources in the pre-launch OD analysis. Shortly after launch, a turn ΔV calibration was performed to measure the amount of residual ΔV. The calibration showed the actual ΔV per turn to be much less than the pre-launch estimate, which contributed to a reduction in the OD uncertainty prior to each maneuver. The MER-A residual turn ΔV was estimated from the calibration to be approximately 0.05 mm/sec per axis for a ten-degree turn. The corresponding MER-B estimate was slightly larger reaching 0.1 mm/sec for the out of trajectory plane component. A more detailed description of this activity can be found in Ref 2.

The solar radiation pressure model consisted of three components models representing the major sections of the spacecraft that were contacted by sunlight. Figure 5 shows the spacecraft and its major sections.

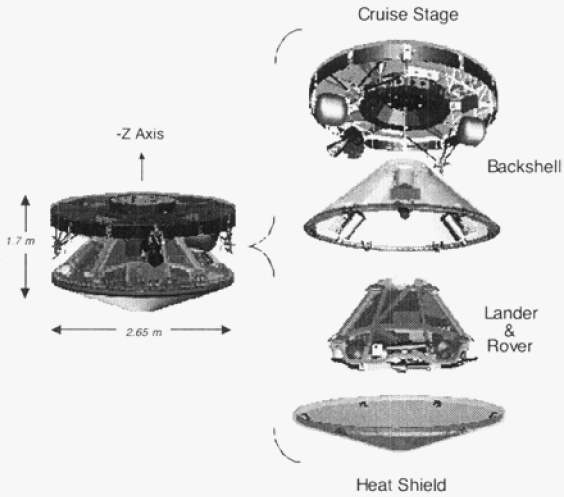

Figure 5. Spacecraft Diagram

The spacecraft was generally pointed with its –Z-axis towards the Earth, which allowed sunlight to contact the top of the cruise stage (solar arrays, launch vehicle adaptor, and heat rejection panels), and the backshell. The model included a cylindrical component that combined the nearly cylindrical HRS panels surrounding the cruise stage with the cylindrical-like shape of the heat shield at the point where the heat shield mates with the backshell. The second and largest component model was a flat plate model, which represented the top of the cruise stage including the solar arrays and launch vehicle adaptor plate. The third component was the conical backshell that was partially shaded by the cruise stage. The conical backshell and shading were modeled with a look up table that was a function of solar aspect angle. Figure 6 shows the shading and reflection of the backshell.

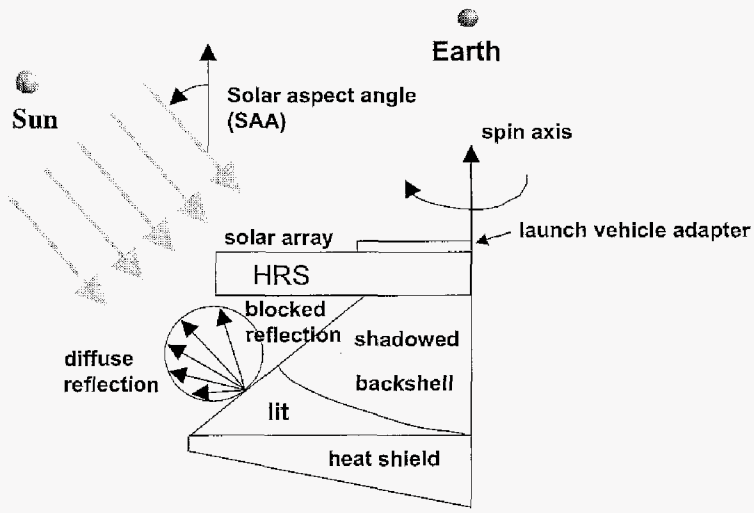

Figure 6. Solar radiation pressure diagram showing the solar aspect angle effect on shading

The navigation team used information about the component physical properties and spacecraft thermal properties to estimate the effective reflectivity coefficients of each component. A more detailed description of this model can be found in Ref. 2.

The addition of ΔDOR measurements to the OD solutions for TCM-2 and TCM-3 helped tremendously in the verification of the aforementioned models. ΔDOR is an interferometric measurement using two antennas at different DSN complexes simultaneously to record the one-way tones from the spacecraft. After the spacecraft recording is complete both antenna slew to simultaneously record signals from a quasar. Both of these recordings are then processed or correlated to produce an angular measurement of the spacecraft relative to the quasar along the DSN complex baseline. After differencing the measurements between the two DSN complexes, removing common error sources, the measurement is a highly accurate measure of position (approximately 4.5 nanoradian angular accuracy in the plane of sky). The Doppler and ranging data measures position and velocity along the line-of-site to the spacecraft while ΔDOR measures position in the plane-of-sky which is perpendicular to the line-of-site. This combination of data types nearly produces a three-axis measurement of the spacecraft position (see Figure 7).

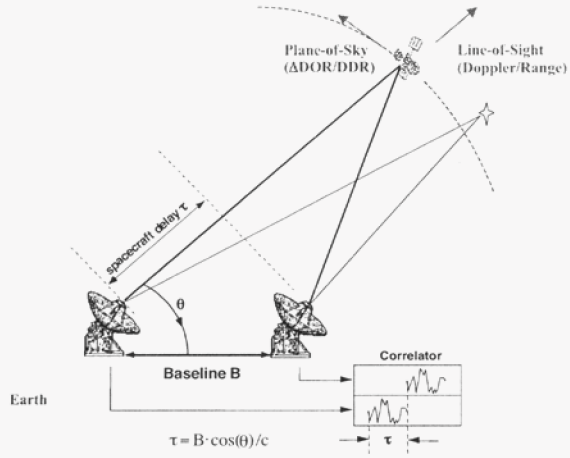

Figure 7. ΔDOR measurement diagram[3]

The combination of two-way Doppler data, range data, and ΔDOR data, along with the performance of the turn ΔV and solar pressure dynamic models allowed the OD analysts to identify an error in the location of one of the DSN antennas. When measuring the position and velocity of the spacecraft, one is actually measuring the position and velocity of the spacecraft at a specific time relative to the antenna transmitting and receiving the data. The normal OD process relies on calibrated positions of the each individual antenna in order to calculate the position of the spacecraft relative to other bodies such as the Earth or Mars. The antenna positions on the Earth are independently estimated by taking very long baseline interferometric measurements (VLBI) of quasars with other antennas at the same and different DSN complexes. With enough data these are very accurate measurements, estimating the position of an antenna can be accomplished to within centimeters. The antenna position uncertainty is normally added into the OD filter as a consider parameter to aid in statistical uncertainty modeling. In the case of MER, DSN station number 26 at the Goldstone complex had a position error of over 60 cm. This station location error was identified by not being able to fit the tracking data from station 26 along with the data from other stations. Figure 8 shows the inconsistency in the station 26 data. The OD analysts estimated the location of station 26 and found that it was in error. Additional independent VLBI measurements using station 26 produced a new estimate that agreed with the OD solutions for the station and allowed all the tracking data to be fit consistently. The results of the OD solution relative to the independent VLBI solution can be seen in Table 2.

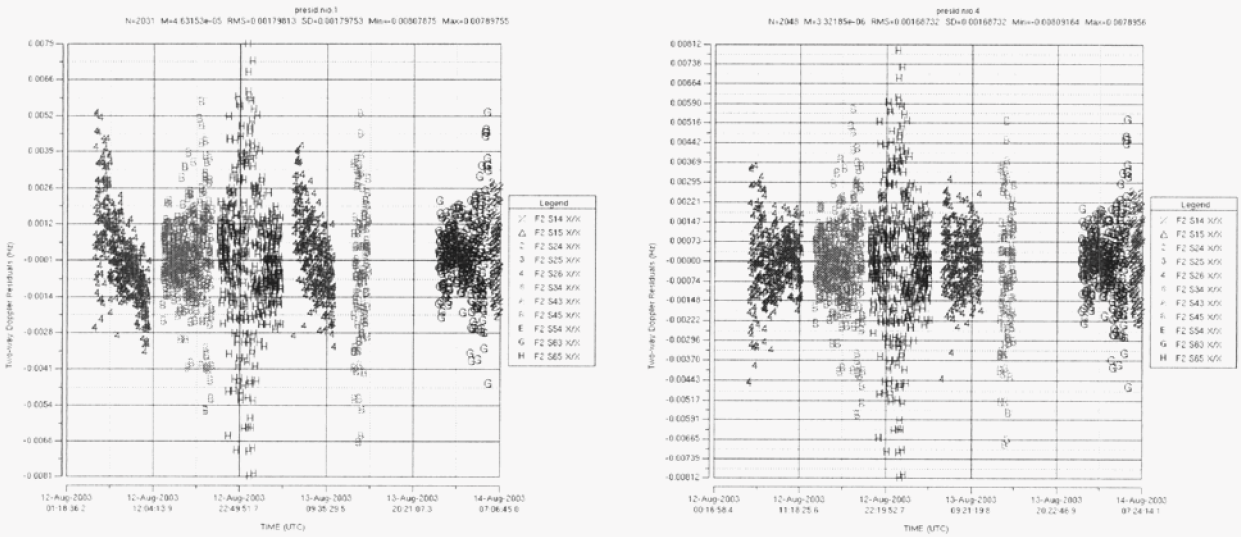

a b

Figure 8. a. Two-way Doppler residuals showing DSN station 26 location error
b. Two-way Doppler residuals with the correct station location

Table 2. Position estimates of DSN station 26 at the Goldstone complex5

	Initial Position	
	Position	1σ uncertainty
Longitude (degrees)	243.1269849	5.2E-07
Height above equator (m)	3668.87221	7.1E-05
Spin Axis distance (m)	5209.76697	8.7E-05

	MER OD Estimate		Final Independent Estimate	
	Estimated Difference	1σ uncertainty	Estimated Difference	1σ uncertainty
Longitude (degrees)	-3.60E-08	5.85E-07	1.40E-06	4.14E-07
Height above equator (cm)	34.4	16.9	45.7	3.4
Spin Axis distance (cm)	61.7	8.1	61.7	3.0

IV. Final Approach Orbit Determination

The primary goal of approach orbit determination was to refine the models such that the spacecraft could be delivered to the atmospheric interface point (Mars radius of 3522.2 km) with an entry flight path angle (FPA) of −11.5 deg ±0.12 deg (3σ) for MER-A and ±0.14 deg (3σ) for MER-B. Satisfying the above conditions was a major factor in successfully landing both spacecraft in their respective landing ellipse. The data types used in the approach phase consisted of two-way Doppler, two-way range, and delta-differenced one-way range (ΔDOR).

A. OD Model Refinements

There were two main model refinements during the approach phase. The first model was incorporated to account for X-band signal delay due to interplanetary solar plasma. There were a few times during the cruise phase when the Doppler data displayed a signature over a pass with increased data noise (Fig. 9). Since the incidents were isolated, these passes were de-weighted in the solution and attributed to increased Earth ionosphere activity. Starting with the approach phase the number of tracking passes was increased from three tracks per week to two tracks per day and then in the last three weeks it was increased to nearly continuous coverage. With the increased tracking coverage it was revealed that during a period of high Doppler noise the signature that was present would persist into subsequent passes at different DSN complexes. This persistence is not a characteristic of Earth ionosphere activity. It was also discovered that this degraded data would occur about every twenty-eight days and the range data had the opposite slope as the Doppler data. The twenty-eight day period is consistent with the period of the rotation of the Sun's equator and the slope information points to signal delay. Furthermore, data degradations of this type were witnessed on MER-A, MER-B and other spacecraft. This commonality suggests a solar plasma effect. A model was developed that applied signal delay corrections to the oppositely sloped Doppler and range data periods. This model helped to smooth out the signatures in the data and helped with solution consistency but it could not reduce the inherent data noise associated with those periods. In order to mitigated this problem a weight by pass process was employed to the data. As the data was received each pass of data was weighted at a scale factor times the RMS of the data noise. A scale factor of 3.36 was applied to the Doppler RMS and a scale factor of 2,22 was applied to the range data. The scale factor was applied in order to mitigate effects related to data noise and data compression.

MER-A

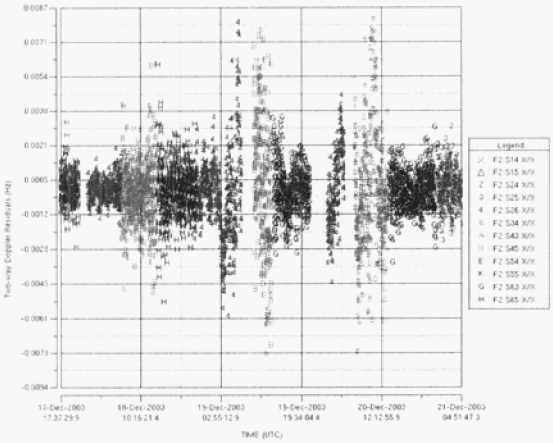

MER-B

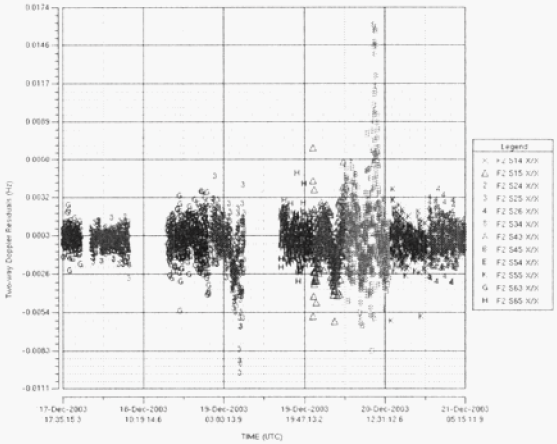

Figure 9: Solar Plasma Effects on Doppler Data

The second major model that was refined was the maneuver execution error and estimation model for TCM-4. Three TCMs (TCM-4, TCM-5, TCM-6) were planned during the approach phase for both spacecraft. TCM-4 at entry minus eight days was used to clean up OD and execution errors that were propagated from TCM-3 and to precisely target the entry conditions. The purpose of TCM-5 at entry minus two days was to further refine the targeting after TCM-4 with the latest OD knowledge to meet the entry interface FPA requirements. TCM-6 at entry minus four hours was only planned for use in case there was a major error in the OD that was realized as the spacecraft reached deep enough into the Mars gravity well. The OD process starts off with a nominal model for the maneuver and its related uncertainty. Once data is acquired after the maneuver, the maneuver parameters are estimated in the OD process. For TCM-1 through TCM-3 the thrust or magnitude along with the right ascension and declination of the ΔV direction were estimated. There were only six days in between TCM-4 and TCM-5, which did not allow for much time to solve for all the directions of the maneuver. In particular, the out-of-plane portion of the maneuver is difficult to estimate in a short amount of time. For MER-A and MER-B the amount of data strength to resolve small velocity variations in the out of plane direction was limited, which caused the OD solutions to vary in that direction (Figure 10). By looking at the past TCMs and ACS turns the *a priori* error was bounded by values much less than the official requirements. The a priori error was bounded by estimating the V direction based on cone and clock angles about the V instead of right ascension and declination. Based on previous maneuvers and the design of TCM-4 the cone angle was constrained. This issue was exasperated for MER-B because the cancellation of TCM-3 caused TCM-4 to be larger in magnitude, causing larger than expected execution errors. As tracking data was accumulated after TCM-4 for both missions, it was apparent in the final hours prior to TCM-5 that bounding the TCM-4 execution errors was the correct action.

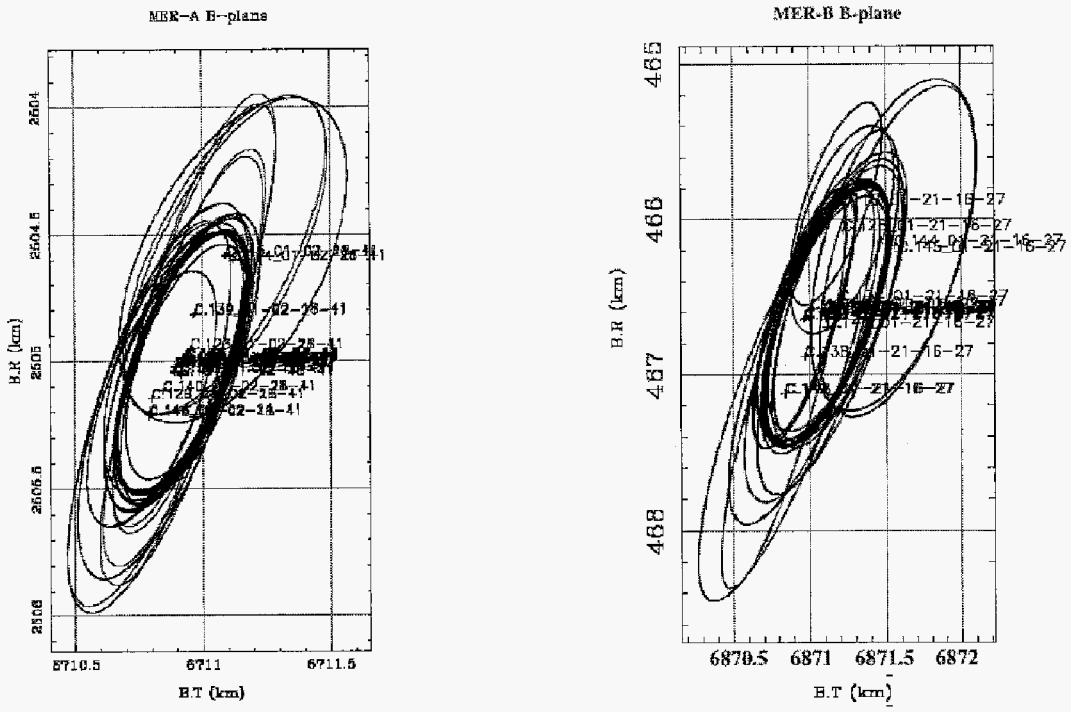

Figure 10. B-plane plot showing a variation of solutions in the out-of-plane direction, the direction that is least visible after a TCM

B. Operational Aspects

In addition to model refinements the final approach phase was filled with detailed operational planning and execution. The main drivers on the OD operational timeline were the amount of time in between the tracking data cutoff and maneuver execution, the number of solutions needed, and the number of operational decision meetings to support. TCM-1 through three used a five day template from the tracking data cut-off to the execution of the maneuver giving OD almost a full day to complete and deliver a solution to the navigation team In the final approach phase the amount of time available for the OD process was reduced to one hour.

Starting at approximately entry minus fifteen days the number of solution deliveries went from one every other day to at least one per day. At this time the navigation team was working prime shift preparing for TCM-4, and the OD analysts would start the day off with a tracking data cutoff at about eight in the morning pacific daylight savings time. The OD team would generate multiple solutions using differing filter estimation strategies and varying the use of the data types. More detail about the types and numbers of solutions can be found in Ref. 6. Once a series of solutions was completed, the team would have a short meeting to discuss which individual solution would be delivered for TCM analysis. Typically the same solution would be delivered multiple days in a row unless additional or improved modeling would cause a case to perform better than the previously delivered case. Major products that were delivered included an updated trajectory, which predicted the spacecraft entry condition, an estimate of the solution uncertainty, and a file, which combined the estimated entry conditions, and uncertainties into a set of dispersed entry conditions. The maneuver analysts would design TCM-4 based on the prediction and the EDL analysts would propagate the dispersed entry states to the Martian surface to evaluate the predicted landing region. Further details about the navigation team processes can be found in Ref 7,8,9. Towards the end of the day the navigation team would hold a series of meetings. The first would be a meeting with the Navigation Advisory Group (NAG), which contained a set of navigation peers from JPL's Navigation and Mission Design section. Other meetings were held to inform the project on the status of the upcoming TCM. The NAG meeting would discuss all aspects of the OD solutions, recommend additional cases or removal of cases, and recommend a particular "best" solution to use for subsequent deliveries.

Starting one day before TCM-5 the OD team started working around the clock using three eight hour shifts (2 analysts per shift) to monitor the data and the trajectory. Each shift would complete at least one set of solutions for monitoring purposes and any additional sets needed for operational meetings or product deliveries. At this time we

set aside two hours to complete a full set of varying OD solutions to be evaluated and only an hour or less for a more focused set of runs immediately prior to an OD delivery. As an example on MER-A on January 2, 2004, the day before TCM-A6 and landing OD analysts completed four full sets of monitoring solution, one smaller set for operational products (EDL parameter update #2[9]) and another full set for a NAG and TCM-A6 status meeting. The landing day was even more complicated with additional sets of operational product runs. This heavily packed timeline was only possible due to the amount of automation built into the navigation processes[3] and the amount of time spent in operational readiness tests (ORT) practicing those processes. During flight the navigation team performed two very detailed ORTs concerning approach navigation and EDL.

C. Final OD Results

Following TCM-4, the estimated entry points for both MER-A and MER-B were well within the required delivery ellipse. In the time between TCM-4 and TCM-5 the OD solutions were extremely stable such that at the time of the scheduled TCM-5 decision meeting the MER-A FPA results were -11.49 ±0.028 (3σ), well within the ±0.12 prediction. The MER-B FPA results were –11.46 ±0.034 (3σ), well within the ±0.14 prediction. At the time of the TCM-5 decision point both spacecraft were well within the desired FPA corridor, predicted to be well within the desired landing ellipse, and the uncertainties were well better than predicted, it was decided to cancel those maneuvers.

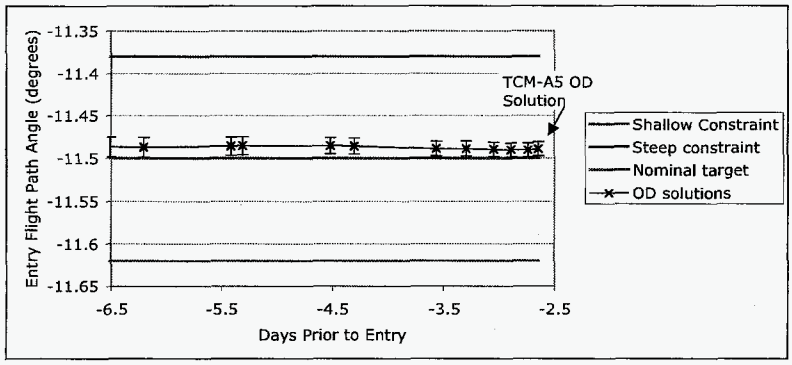

a.

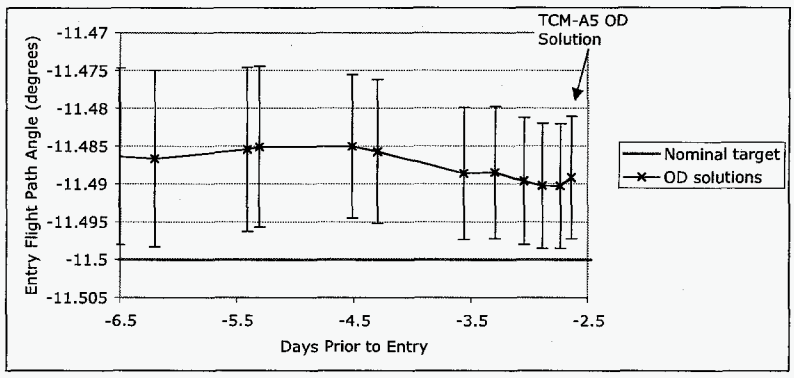

b.

Figure 11. Entry flight path angle solution history
a. Shows the solution FPA relative to constraints
b. Show the solution FPA variation from TCM-4 to TCM-5

TCM-6 was scheduled to be executed only in the case where there was a gross OD modeling error which was realized late in the trajectory, within one day of entry as the gravity of Mars significantly affected the spacecraft and dominated the dynamics. The OD solutions were very stable in the time between the TCM-5 decision and the TCM-6 decision. The MER-A entry FPA estimate only differed 0.005 from the TCM-A5 decision value during the time from the TCM-A5 decision to the TCM-A6 decision. The MER-B FPA estimate only varied 0.001 deg from the

TCM-B5 decision value. Again both spacecraft were well within the FPA corridor; no gross OD modeling errors existed, and therefore no TCM-6 maneuver was executed on either spacecraft (Fig. 12).

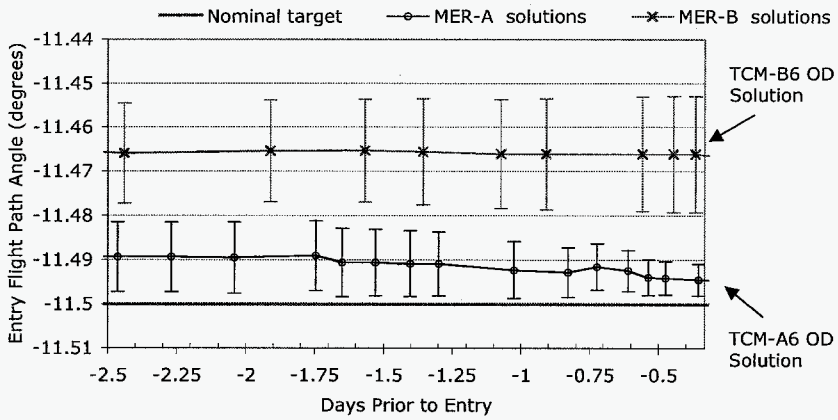

Figure 12. MER-A and MER-B entry flight path angle solutions from the TCM-5 decision point to the TCM-6 decision point

Another use of the OD solutions was to update the parameters used in the spacecraft entry, descent, and landing (EDL) software. The algorithms used in the EDL software (software on board the spacecraft which triggered critical deployments such as the parachute) depended on the estimated time of entry, the entry FPA, and the entry FPA dispersion. The operations team scheduled multiple opportunities to update the EDL parameters during the approach phase. The parameter updates were normally scheduled after TCMs so that as soon as the trajectory was changed due to a TCM the EDL parameters were updated to reflect that change. As TCM-5 and TCM-6 were canceled the EDL parameter updates remained and the decision of whether or not to update the spacecraft's parameters was made after new parameters were calculated based on the latest OD solution. The OD solutions were stable enough so that no EDL parameter updates were made based on changes in entry state estimates. All the updates were due to either refinement in the atmosphere model or in the EDL system modeling.

V. Conclusion

After seven months of travel and four trajectory correction maneuvers on MER-A and only three trajectory correction maneuvers on MER-B, the MER navigation team delivered each spacecraft safely to there corresponding atmospheric interface points to within -0.007 ±0.0099 deg (3σ) for MER-A and 0.03 ±0.021 deg (3σ) for MER-B. During interplanetary cruise, the OD uncertainty results were well within pre-launch predicted values, which allowed the team to identify a DSN station location error, estimated for solar plasma effects on the data, and refine the spacecraft dynamic models. All of this effort paid off ten fold on January 3 and January 24, 2004 when the Spirit and Opportunity spacecraft safely landed on the surface of Mars only 9.7 km and 24.6 km down range of their respective targets[9].

Acknowledgements

This research was carried out at the Jet Propulsion Laboratory, California Institute of Technology, under a contract with the National Aeronautics and Space Administration.

Reference herein to any specific commercial product, process, or service by trade name, trademark, manufacturer, or otherwise, does not constitute or imply its endorsement by the United States Government or the Jet Propulsion Laboratory, California Institute of Technology.

References

[1] Portock, B.M., "Mars Approach Navigation Challenges," Paper AIAA 2000 -4425, *AIAA/AAS Astrodynamics Specialist Conference*, Denver, CO, 14-17 August 2000.

[2] Kangas, J. A., Potts, C. L., and Raofi, B., "Mars Exploration Rovers Launch Performance and TCM-1 Maneuver Design," *AIAA/AAS Astrodynamics Specialist Conference*, AIAA-2004-4984, AIAA, Washington, DC, 2004.

[3]Wawrzyniak, G. G., Baird, D. T., Graat, E. J., McElrath, T. P., Portock, B. M., and Watkins, M. M., "Mars Exploration Rovers Orbit Determination System Modeling," *AIAA/AAS Astrodynamics Specialist Conference*, Providence, AIAA-2004-4983, AIAA, Washington, DC, 2004.

[4]Portock, B.M., D'Amario L.A., Haw R.J., "2003 Mars Exploration Rover Orbit Determination using ΔVLBI Data," Paper AIAA 2002 -4814, *AIAA/AAS Astrodynamics Specialist Conference*, Monterey, CA, 5-8 August 2002.

[5]Folkner, W. M. and Jacobs, C. S., "DSN Station Location Update for MER," Tech. rep., Jet Propulsion Laboratory, Pasadena, CA, Oct. 2003.

[6]McElrath, T. P., Watkins, M. M., Portock, B. M., Graat, E. J., Baird, D. T., Wawrzyniak, G. G., Guinn, J. R., Antreasian, P. G., Attiyah, A. A., Baalke, R. C., and Taber, W. L., "Mars Exploration Rovers Orbit Determination Filter Strategy," *AIAA/AAS Astrodynamics Specialist Conference*, AIAA-2004-4982, AIAA, Washington, DC, 2004.

[7]D'Amario, L. A., "Mars Exploration Rovers Navigation Results," *AIAA/AAS Astrodynamics Specialist Conference*, AIAA-2004-4980, AIAA, Washington, DC, 2004.

[8]Potts, C. L., Raofi, B., and Kangas, J. A., "Mars Exploration Rovers Propulsive Maneuver Design," *AIAA/AAS Astrodynamics Specialist Conference*, AIAA-2004-4985, AIAA, Washington, DC, 2004.

[9]Knocke, P. C., Wawrzyniak, G. G., Kennedy, B. M., Parker, T. J., Golombek, M. P., Duxbury, T. C., Kass, D. M., and Desai, P. N., "Mars Exploration Rovers Landing Dispersion Analysis," *AIAA/AAS Astrodynamics Specialist Conference*, AIAA-2004-5093, AIAA, Washington, DC, 2004.